Visible Light Up-conversion of Bio-Carbon Quantum-Dot-Decorated TiO2 for Naphthalene Removal

Yunteng Chen , Chunxian Hong , Qiang Xu , Haihong Zheng , Chao Wang , Hongshun Lu , Shuai Zhang , Mingming Du * , Ganning Zeng *

Posted Date: 17 April 2024

doi: 10.20944/preprints202404.1092.v1

Keywords: Carbon quantum dots; TiO2; Photodegradation; Naphthalene

Article

Visible Light Up-conversion of Bio-Carbon Quantum-Dot-Decorated TiO_2 for Naphthalene Removal

Yunteng Chen [1,2], Chunxian Hong [3], Qiang Xu [4], Haihong Zheng [5], Chao Wang [4], Hongshun Lu [4], Shuai Zhang [4], Mingming Du [3,*] and Ganning Zeng [2,*]

[1] Shaoxing Communications Investment Group Co., Ltd., 312099 Shaoxing, Zhejiang, China; cccpa@aliyun.com (Y.C.);
[2] College of Environment, Zhejiang University of Technology, 310014 Hangzhou, Zhejiang, China
[3] College of Chemical Engineering, Zhejiang University of Technology, 310014 Hangzhou, Zhejiang, China; 15858239167@163.com
[4] China Construction Third Engineering Shanghai Co., Ltd,200082 Shanghai, China; 124056@cscec3b.com.cn(C.W.); 118712@cscec3b.com.cn (H.L.); 135506@cscec3b.com.cn (S.Z.)
[5] Hangzhou Construction Quality and Safety Supervision Station, 310012 Hangzhou, Zhejiang, China; 104309@cscec3b.com.cn
* Correspondence: dwentrance@zjut.edu.cn (M.D.); gnzeng@zjut.edu.cn (G.Z.)

Abstract: In this study, carbon-quantum-dot (CQD)-decorated TiO_2 was prepared using an ultrasonic doping method and applied in the photocatalytic degradation of naphthalene under sunlight irradiation. The CQDs were synthesized from a typical macroalgae via diluted sulfuric acid pretreatment and hydrothermal synthesis using an optimal design, i.e., 3 wt% and 200 °C, respectively. The CQD/TiO_2 composite remarkably enhanced the photocatalytic activity. The degradation of naphthalene under a visible light environment indicated that there is a synergistic mechanism between CQDs and TiO_2, in which the generation of reactive oxygen species is significantly triggered; in addition, the N that originated from the macroalgae accelerated the photocatalytic efficiency. Kinetic analysis showed that the photo-catalytic behavior of the CQD/TiO_2 composite followed a pseudo-first-order equation. Consequently, our combined experimental approach not only provides a facile pretreatment process for bio-CQDs synthesis, but also delivers a suitable TiO_2 photocatalyst for up-conversion, along with critical insights into the development of harmful macroalgae resources.

Keywords: carbon quantum dots; TiO_2; photodegradation; naphthalene

1. Introduction

Polycyclic aromatic hydrocarbons (PAHs) have teratogenic, carcinogenic, and mutagenic effects that likely threaten human health via bio-communication or the amplification of the food chain [1]. Among the diverse remediation technologies that can be applied to aquatic PAHs, TiO_2 photocatalysis has garnered attention in recent years due its good photochemical stability, high catalytic efficiency and strong capacity for oxidation [2,3]. However, due to its wide band gap and high photo-generated electron–hole pair recombination rate [4], unmodified TiO2 is often less active in the visible region and exhibits low carrier utilization; these factors greatly limit its widespread application.

Many research endeavors have been dedicated to developing modified TiO2 photo-catalyst systems in order to maximize the utilization of visible light [5]; in these, carbon doping technologies have been found to help overcome some of the intrinsic shortcomings of TiO2, such as its low absorption and utilization of light, and to easily recombine photo-generated electrons and photo-generated holes [6]. Compared to other technologies utilized for the doping of carbon materials,

 doi:10.20944/preprints202404.1092.v1

CQDs are particularly attractive in this field due to their capacity for electron transfer, good photo-luminescence, up-conversion fluorescence performance, and facile tunability [7,8]. However, the top-down method utilized for the preparation of CQDs still has certain limitations; for example, the carbon precursors are usually limited to materials with a large area of sp2 hybridization. In comparison, the bottom-up synthesis method employed for the preparation of CQDs has been widely used due to its simplicity and practicability [9,10]. It is worth noting that the development of simple, low-consumption and gentle synthetic methods for the preparation of fluorescent CQDs and the use of readily available, inexpensive and environmentally friendly natural resources as green carbon precursors has become an active research area. Biomass, especially renewable biomass materials, has been widely used as a precursor for the preparation of CQDs, showing good photo-luminescence properties, low toxicity and good bio-compatibility [11,12]. However, its practical application is hindered by its low yield, low fluorescence intensity, and controllability, which are affected by its complex biological composition. Therefore, the preparation of CQDs from biomass, especially waste biomass, has become a research hotpot in recent years. With this in mind, a fast-growing macro-algae, i.e., *Sargassum Horneri* (*S.H.*), whose burst is defined as golden tide [13] was used as a CQD precursor.

On the other hand, the synergistic effect of CQD/TiO_2 has been proven to effectively inhibit the recombination of electrons and holes and improve the photo-catalytic efficiency [14]. In CQD/TiO_2 composites, CQDs are bonded to TiO_2 by Ti-O-C bonding, and some electrons migrate to TiO_2; this results in Ti^{3+} defects in the TiO_2 matrix and a positive charge on the surface of the CQDs. As a result, Ti^{3+} can promote the adsorption of O^{2-} on the surface of the photo-catalyst. Meanwhile, the excited electrons of the composites can be transferred from the valence band (VB) of the CQDs to the conduction band (CB) of TiO_2. Sequentially, the electrons of CB in TiO_2 react with O_2 to form·O^{2-}, and the holes on the surface of the CQDs further oxidize H_2O to form ·OH free radicals; these two free radicals play a role in the degradation of contaminants. In addition, some visible light can be collected and up-converted into photons with a higher energy via CQDs. As an important electron reservoir, CQDs can collect and store photo-generated electrons from the CB of TiO_2, thereby hindering the recombination of electron–hole pairs and further promoting photo-catalytic activity. Regarding TiO_2, its light response generally ranges within the ultraviolet light region and is excited with difficulty by light sources larger than 420 nm because of the wide band gap. Meanwhile, CQDs can effectively up-convert visible light that has a wavelength greater than 420 nm into ultraviolet and near-ultraviolet light with a range of 350–550 nm [15,16]. Under light irradiation, the photo-generated electrons trapped on CQDs can further reduce the absorbed O_2 to reactive ·O^{2-}, the generation of which may depend on the separation efficiency of the photo-generated carriers and the number of photo-generated electrons captured by the CQDs. In particular, due to their graphite-like electronic structure and functional groups, CQDs can promote the adsorption of organic compounds by the complex, improve the area of contact with the target contaminants, and further carry out the photo-degradation process. It is worth mentioning that the measurement of the transport band gap of the CQDs and TiO_2 is also crucial, as the optical properties, the separation, and the migration of electrons in photo-catalysts are the key factors that determine the photo-catalytic activity [17–19].

The surface of biomass CQDs is rich in oxygen-containing functional groups [20–22]; they are therefore able to combine with semiconductors such as TiO2 to form potential photo-catalysts. In recent years, algae and their derived carbon materials have been found to act as co-catalysts when coupled with TiO2 [23–25]. However, CQD/TiO2 photo-catalysts prepared using biomass are also affected by their complex biological composition. A suitable pretreatment method would destroy the cellulose of the natural plant structure and increase the specific surface area and porosity of the raw materials; therefore, the economic and facile pretreatment of biomass for sequential composite synthesis is still crucial and challenging. In order to improve the yield of carbon quantum dots, dilute acid can be used in the pretreatment of biomass, showing the ability to perform cellulose hydrolysis under relatively wild reaction conditions [26,27]. Therefore, the steps of our reaction are defined as follows: pretreatment with dilute acid, the hydrothermal preparation of CQDs, and the synthesis of CQD/TiO_2 via ultrasonic dipping. Furthermore, the potential of CQD/TiO_2 as a photo-catalyst was investigated in the aquatic degradation of naphthalene under visible light. The aims of this study

 doi:10.20944/preprints202404.1092.v1

were to build a facile pretreatment process for bio-CQDs synthesis, to obtain a suitable method for the visible light up-conversion of a bio-CQD-decorated TiO_2 catalyst, and to find a potential industrial application for macroalgae.

2. Materials and methods

2.1. Materials

S.H. was collected from Wenzhou coastal area and washed with deionized water to remove salts and impurities on the surface, before being dried in an electric blast oven for 24 h. The dried *S.H.* was then ground and sieved through an 80-mesh sieve. Reagents were acquired from commercial suppliers and used without any further processing or purification. Titanium dioxide (P25, Degussa, 99.5%) was procured from Sinopharm Chemical reagent Co., Ltd., and chromatographic pure naphthalene was purchased from Aladdin Reagent Company. Analytically pure acetic acid, sulfuric acid (H_2SO_4), hydrochloric acid (HCl), sodium hydroxide (NaOH) and dichloromethane were purchased from Lingfeng Chemical Reagent Co., Ltd (Shanghai, China).

2.2. Preparation of CQDs and CQD/TiO_2

Dilute sulfuric acid was dissolved using 50 mL of de-ionized water in a 100 mL beaker, and the solution was transferred to a 100 mL stainless steel reactor; it was then placed in a drying oven at a predetermined temperature for 3 h. After the reaction, the CQD solution was cooled to room temperature. Then, centrifugation was performed 3 times at a speed of 10000 $r \cdot min^{-1}$ to remove the large particles; this was followed by neutralization and separation using a 0.22 μm polyethersulfone membrane. Sequentially, the carbon quantum dot (CQD) solution was obtained and designated as CQDs(L) (L means liquid) (Figure S-1 in Supplementary material). The CQD solution was freeze-dried to obtain a solid powder of CQD; this was as designated as CQDs(S) (S means solid).

2.3. Characterization of CQDs and CQD/TiO_2

The morphology, size and crystal lattice of the materials were analyzed using transmission electron microscopy with a Field Emission Gun (TEM, Tecnai G2 F30, FEI). In detail, the parameters were as follows: the excitation voltage was 300 kV, the line resolution was 0.1 nm, the point resolution was 0.2 nm, and the information resolution was 0.14 nm. A Fourier transform infrared spectrometer (FT-IR, Nicolet IS50) was used in the range of 400-4000 cm^{-1} with a resolution of 4 cm^{-1} to characterize the surface function groups of the composites. UV-Vis absorption measurements were carried out via UV-Vis diffuse reflectance spectrophotometry (DRS) (CARY 300, Agilent), with scanning in the range of 200-800 nm. The obtained data were processed according to the Tauc plot method. The surface chemical composition and chemical status of the CQD/TiO_2 were investigated using X-ray photoelectron spectroscopy (XPS, Kratos Axis-Ultra). In this paper, Al/Mg was used as the radiation source. The test conditions were as follows: the excitation source was Al Kα (1487 eV), the target voltage was 15 kV, the current was 3 mA, the vacuum degree was 10^{-7} Pa, and the binding energy was corrected with C1s and a reference of 284.6 eV.

2.4. Photo-catalytic activity measurements

The photo-catalytic activity of the CQD/TiO_2 composites was evaluated using naphthalene. The photo-degradation experiments were performed by using a photochemical reactor (PhChem-III, Newbit Technology Co., Ltd., China) equipped with a Xenon arc lamp (500W, XE-JY500) to simulate sunlight irradiation. The catalysts were added to 10 mL of naphthalene solution (40 mg L^{-1}) and stirred for 60 min under dark conditions to ensure that adsorption–desorption equilibrium was reached before photo-catalysis was performed. During the photo-catalysis process, the concentrations of naphthalene were determined using gas chromatography (GC-112A, Shanghai Yidian Analytical Instrument Co., Ltd., China) , and the relative removal rate ® of naphthalene was calculated based on triplicate experiments in an air-conditioned room to prevent heat effects. The

 doi:10.20944/preprints202404.1092.v1

detection conditions were as follows: the column used was the Agilent DB-5 capillary column (30 m × 0.32 mm × 0.25 μm); the detector used was a hydrogen flame ionization detector; the detector temperature was 280 °C; the inlet temperature was 250 °C; the column temperature was programmed to be maintained at 60 °C for 1 min, 4 °C·min¹ to 130 °C for 5 min, and then 20 °C·min^{-1} to 280 °C; the carrier gas used was high-purity nitrogen, with a flow rate of 2.5 mL·min^{-1}; the hydrogen flow rate was 40 mL·min^{-1}; and the air flow rate was 400 mL·min^{-1}. The gas chromatography results were presented using the internal standard–standard curve method.

3. Results and discussion

3.1. Effect of dilute sulfuric acid pretreatment on CQDs

The pretreatment with dilute acid was performed to hydrolyze and destroy the natural plant structure of the cellulose and simultaneously increase the specific surface area and porosity of *S.H.* [28], as well as the yield of CQDs. This method is more convenient compared to both the traditional method using concentrated acid, from the viewpoint of contamination, or the method using ultra-low dilute acid, from the viewpoint of energy demand; this is due to the high temperature and pressure that this method requires. Based on the results, an optimized design was chosen, i.e., 3.0% H_2SO_4 and a hydrothermal condition of 200 °C; with this, there was an almost 10-fold increase in the CQD yield , rising from 2.3% to 18.9% (Figure S-2, S-3 in Supplementary Materials). Regarding the synthesis of the CQD/TiO_2 nano-composite, 0.40 g of TiO_2 and 1-10 mL of the CQDs(L) (Liquid form, abbreviated as L), in which 1 mL of CQDs(L) corresponded to 0.012 g of CQDs(S), were dispersed into 30 mL of deionized water and processed using ultrasonic irradiation for 30 min. The suspension was dried at 60 °C for 24 h to achieve a CQD/TiO_2 composite.

3.2. Characterization of CQDs and CQD/TiO_2

The TEM analysis indicated that the CQDs presented an approximately spherical nano-morphological distribution with a nanometer size. The CQDs had a good in-plane lattice with a spacing of 0.283 nm (Figure 1a), which is close to the (101) plane of graphite. The CQD/TiO_2 had a good crystal plane spacing that was similar to that of TiO_2, and the diameter of the CQDs had no obvious effect on the morphology of TiO_2. This indicates that there was a good binding structure between the CQDs and TiO_2. Meanwhile, after embedding CQDs into TiO_2, the lattice spacing of the CQD/TiO_2 composite was determined to be 0.328 nm (Figure 1b).

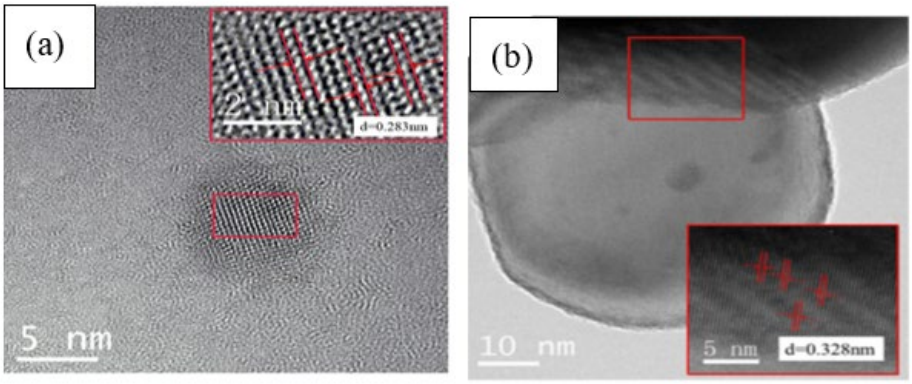

Figure 1. TEM image of CQDs and CQD/TiO_2: (a) 5 nm; (b) 10 nm.

3.2. UV-Vis Analysis of CQD/TiO_2

In the ultraviolet wave band, the light absorption of CQD/TiO_2 is less than that of TiO_2, but in the visible light region, the light absorption of the CQD/TiO_2 composite material is greatly enhanced compared to that of TiO_2 (Figure 2). Because the CQDs exhibit a higher LUMO (Lowest Unoccupied Molecular Orbital)) energy level than the TiO_2, the electrons excited by visible light can be easily transferred from the LUMO energy level to the CB of TiO_2, and the absorption intensity of the

 doi:10.20944/preprints202404.1092.v1

CQDTiO2 is much higher than that of TiO2 in the visible region [29]. The threshold wavelengths (λg) of the absorption spectra of simple TiO2 are obviously lower than those of the CQD/TiO2 composite, which is due to the near-infrared absorption characteristics of CQDs [30] (Figure S-4 in Supplementary Material). The light absorption redshift and range broadening significantly indicated the promotion of the photocatalytic performance [31]. Further calculations also showed that the binding energy of the CQD/TiO2 (3.00eV) was lower than that of TiO2 (3.20 eV), which meant that more excited electrons transferred from the VB to the CB; this led to the promotion of the photo-absorption of the composite. That is to say, the up-conversion performance of CQDs and their tight combination with TiO2 can effectively promote the red-shift of the absorption wavelength and effectively inhibit the recombination of electrons and holes.

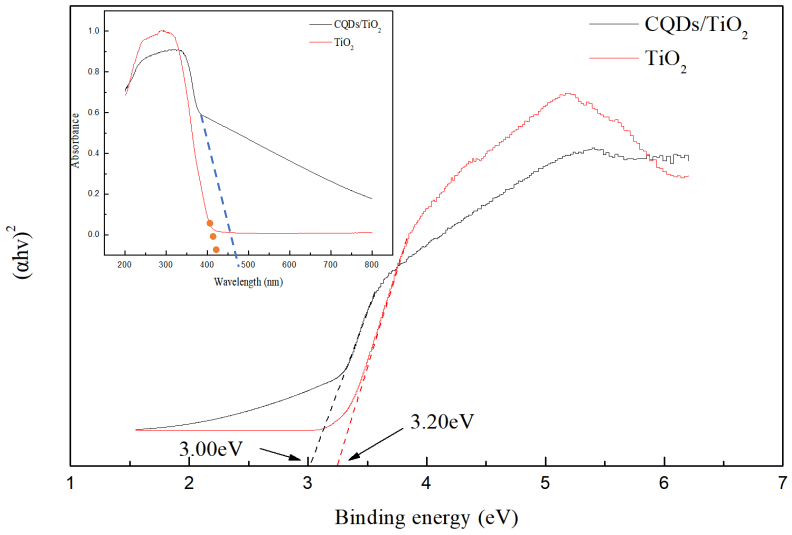

Figure 2. UV-Vis DRS result of CQD/TiO2 composite.

3.3. FTIR Analysis of CQD/TiO2

The FT-IR spectra of different materials are illustrated in Figure 3. In the FTIR spectra, the broad and strong absorption band peak at 3370 cm^{-1} is assigned to the -OH stretching vibration, and the absorption peaks at 2900 cm^{-1} and 1700 cm^{-1} are the stretching vibration peaks of C-H and C=O, respectively. The conjugate characteristic absorption peak produced by C=C appears near 1400 cm^{-1}, and the absorption peak at 650-900 cm^{-1} may be the benzene ring hydrogen absorption peaks of in-plane, out-of-plane and benzene ring skeleton bending vibration. The FTIR analysis indicates that carbonaceous groups were introduced on the surface of TiO2, thus confirming the formation of the CQD/TiO2 composite. Meanwhile, the combination of CQDs enhances the absorption intensity of the Ti-O bond at 1100 cm^{-1}, and this peak is the characteristic absorption peak of the Ti-O bond. In addition, the CQD/TiO2 shows a strong capacity for absorption when the wave number is lower than 1000 cm^{-1}, which may be related to the increased distance between atoms or lattices, and the characteristic absorption peaks of Ti-O-C.

 doi:10.20944/preprints202404.1092.v1

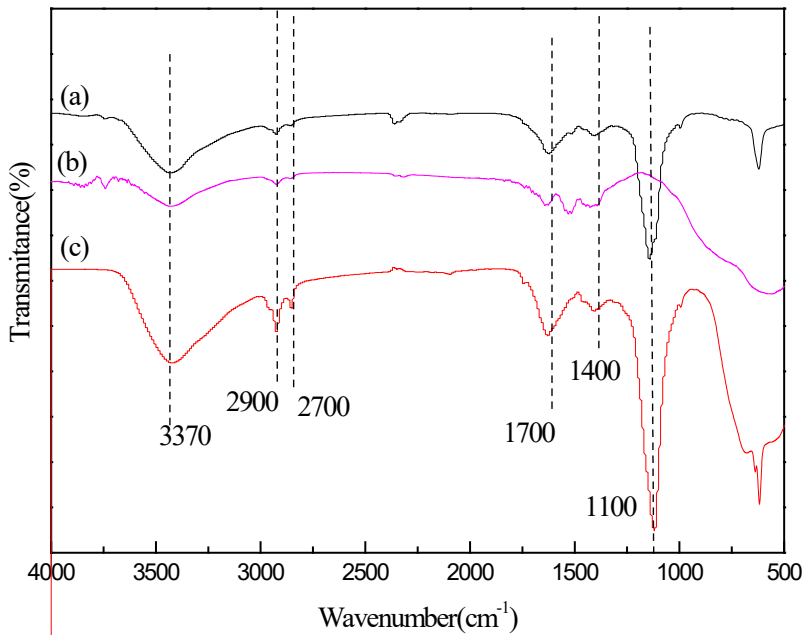

Figure 3. FT-IR spectra of different materials: (a) CQDs (b) TiO_2 (c) CQD/TiO_2.

3.4. XPS analysis of CQD/TiO_2

To explore the surface chemical composition and related valence state of the CQD/TiO_2, the XPS full spectrum is given in Figure 4. Figure 4a shows that the composite contains the elements Ti, O, C, S, and N. The Ti 2p spectrum exhibited two peaks at 454.72 eV and 460.53 eV, which corresponded to Ti 2p3/2 and Ti 2p1/2, respectively; these are assigned to Ti^{4+} 2p peaks [32,33]. The binding energy of Ti 2p is shifted from the standard value of TiO_2, indicating that there is a new binding structure in the CQD/TiO_2 composite. The binding energy of Ti 2p3/2 is lower than the standard value of 458.20 eV, indicating that the existence of CQDs makes the electron binding energy smaller and increases the electron density of TiO_2. Figure 4c shows the C 1s spectrum. The peaks of the C 1s spectrum at 284.32 eV, 285.76 eV, and 288.21 eV are attributed to the C-C/C=C, C-O and C=O bonds, respectively. Figure 4d shows that the absorption peaks of 529.35 eV, 530.72 eV and 532.40 eV in the O 1s spectrum are the characteristic peaks of the Ti-O/·O^2, C=O and C-O groups, indicating the composition of the surface of the CQD/TiO_2 composite material. The peak at 529.35 eV was attributed to the oxygen in the crystal lattice (Ti-O/O^2), and the other two peaks at 530.72 eV and 532.40 eV were attributed to the C=O and C-O groups, indicating that a hybrid might have been formed in the CQD/TiO_2 by a Ti-O-C bond. Figure 4e and Figure 4f show the spectral lines of N 1s and S 2p. The absorption peaks of the N 1s spectrum at 396.50 eV and 398.00 eV are Ti-N and Ti-N-O bonds, respectively. The binding energies of S 2p 3/2 and S 2p1/2 are located at 165.3 eV and 166.8 eV, respectively, mainly due to the S-C-S bond. N and S originated from the biomass, and the latter also was enhanced by the inclusion of the dilute sulfuric acid pretreatment. The doping of N and S also promoted the performance, thus indicating the advantages of biomass self-assembly [34]. In summary, the XPS analysis confirmed the presence of CQDs and their TiO_2 counterparts in the structure of the composites.

 doi:10.20944/preprints202404.1092.v1

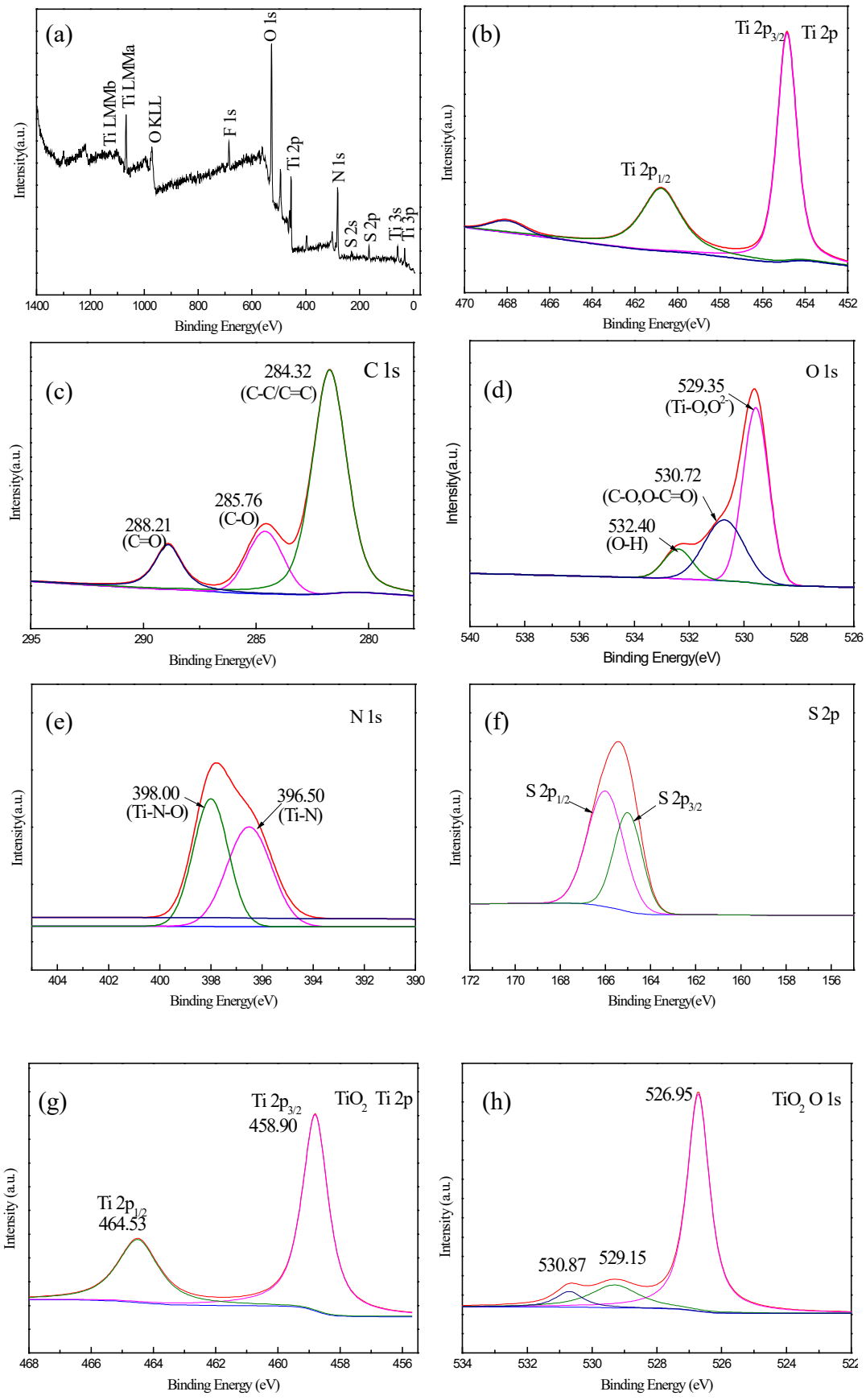

Figure 4. XPS spectra of CQD/TiO_2 composite materials: (a) full spectrum; (b) Ti 2p spectrum; (c) C 1s spectrum; (d) O 1s spectrum; (e) N 1s spectrum; (f) S 2p spectrum; (g) Ti 2p spectrum of TiO_2; (h) O 1s spectrum of TiO_2.

 doi:10.20944/preprints202404.1092.v1

3.5. Photocatalytic Performance of CQD/TiO_2 on Naphthalene Removal

In order to certify the photo-catalytic intensification of CQDs and the dilute acid treatment, the degradation of naphthalene was performed using different materials, as shown in Figure 5. The initial environment parameters were as follows: the naphthalene concentration was 40 mg·L^{-1} and the volume was 500 mL; the CQD/TiO_2 was synthesized using a mixture with a ratio of 10 mL of CQDs to 0.40 g of TiO_2; and 0.03 g of solid material was used. It can be seen that the photo-catalytic effect of CQD/TiO_2 is the best among all the materials, indicating that the doping of CQDs is beneficial to the photo-catalytic performance. The sulfuric acid pretreatment helps the CQDs to promote adsorption, thus leading to their tight combination with TiO_2 and promoting the photo-catalytic performance of CQD/TiO_2.

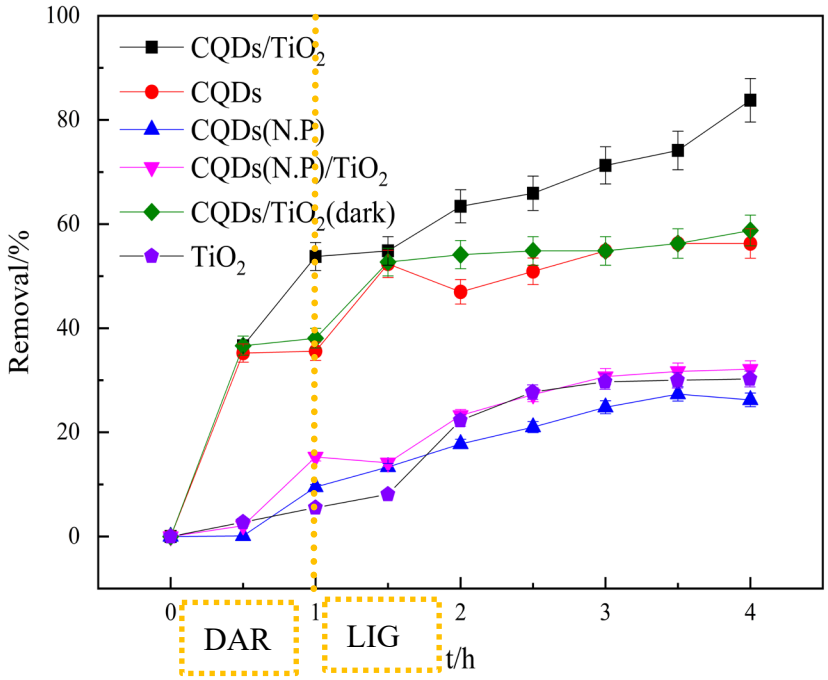

Figure 5 Effect of different materials on photocatalytic reaction of naphthalene (N. P. means without pretreatment using dilute sulfuric acid).

It is worth mentioning that adsorption continued to play an important role regardless of whether the dark or light condition was used; this is because the CQDs continued to mix with biomass carbon. In particular, with the increase in the carbon content, the adsorption of biomass carbon becomes crucial to the formation of the composite; meanwhile, the increase in the proportion of TiO_2 used makes the photocatalytic effect more obvious [28]. It could be found that the number of CQDs in the CQD/TIO_2 composite leads to variations in the removal efficiency; for example, an overdose of CQDs in TiO_2 may cause particle aggregation and pore blocking, and thus reduce the photo-catalytic efficiency (Figure 6-a). This overdose effect was most obvious with the composite mass; the photo-catalytic efficiency of the naphthalene solution was the best, at 86.63%, with the mass of CQD/TiO_2 achieving 0.03 g (Figure 6-b). Regarding the pH effect, the composite catalyst had a good catalytic effect on naphthalene around pH=6 (Figure 6-c), which was greatly affected by TiO_2; this increased the acid–basic balance to pH_{zpc} ~6.39 [35,36]). When the pH value of the reaction system is less than pHzpc, the increase in H+ in the solution will cause Ti-OH^{2+} generation; this is suitable for attracting photo-generated electrons and thereby effectively reducing the recombination rate of photo-generated electrons and holes. The best dose of CQD/TiO_2 could a result of the balance between two aspects, i.e., the active sites involved in the reaction, and the capacity of the receiving photons.

 doi:10.20944/preprints202404.1092.v1

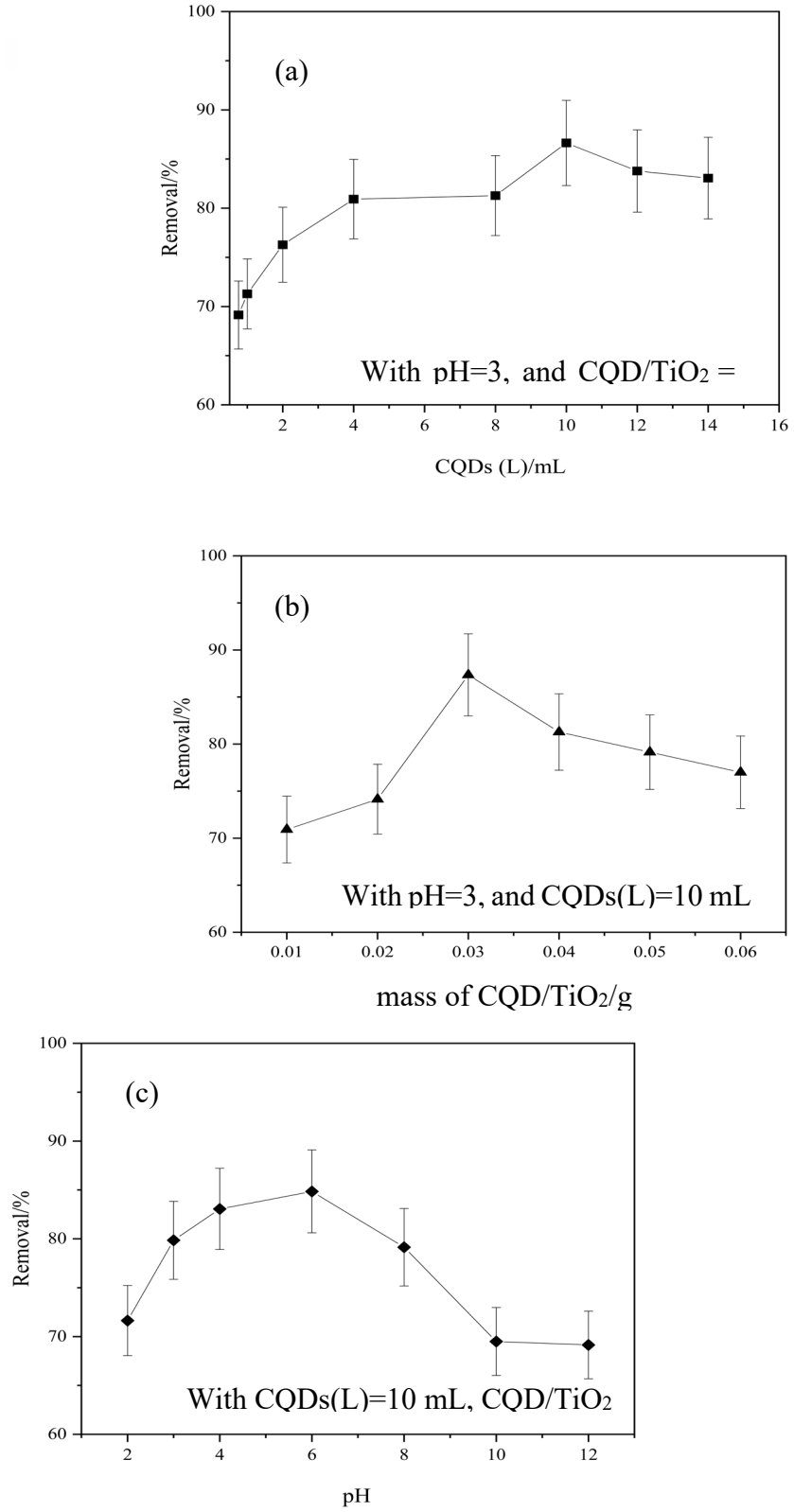

Figure 6. Effect photocatalytic degradation of CQD/TiO_2 on naphthalene.

3.6. Photocatalytic Mechanism Analysis of CQD/TiO_2 on Naphthalene Removal.

In this work, the results of FT-IR, ultraviolet–visible spectroscopy and fluorescence spectroscopy showed that there were abundant functional groups on the surface of the CQD/TiO_2, and that the absorption peaks at wavenumbers lower than 1000 cm^{-1} were the characteristic absorption peaks of

 doi:10.20944/preprints202404.1092.v1

Ti-O-C. The band gap of CQD/TiO_2 was reduced compared with that of TiO_2, and the absorption band shifted to visible light. Furthermore, the XPS results also indicated the variation in the surface elements of the composites, and the results showed that the electron density of the outer layer of Ti increased and the electron binding energy decreased. In addition, the Ti 2p line showed that CQDs and TiO_2 were bonded through Ti-O-C bonds. The mechanism is illustrated in Figure7, i.e., the photo-induced electron transfer and redox properties of CQDs improve the separation time of electron–hole pairs of TiO_2, prevent the recombination of electron-holes. This provides more time for the contaminants to diffuse to the reactive site, which accelerates the photocatalytic efficiency.

CQDs can be used as an electron reservoir during photocatalysis, and the excited electrons of CQD/TiO_2 can be transferred from the valence band (VB) of CQDs to the conduction band (CB) of TiO_2, thereby hindering the recombination of electron–hole pairs and further promoting the photocatalytic activity. The generation of reactive oxygen species (ROS) can be triggered by low-power visible light irradiation [37], i.e., the electrons of CB in TiO_2 react with O_2 to form $\cdot O_2^{-}$. The photogenerated electrons trapped on CQDs can further capture the absorbed O_2 to reactive $\cdot O_2^{-}$, and the holes on the surface of CQDs oxidize H_2O to form ·OH [38,39]. This provides more time for the contaminants to diffuse to the reactive site, which accelerates the photocatalytic efficiency. In addition, the N originating from the biomass makes TiO_2 exhibit p-type conductive properties [40,41], which makes it easier for electrons to transfer to CQDs and improves the photocatalytic efficiency.

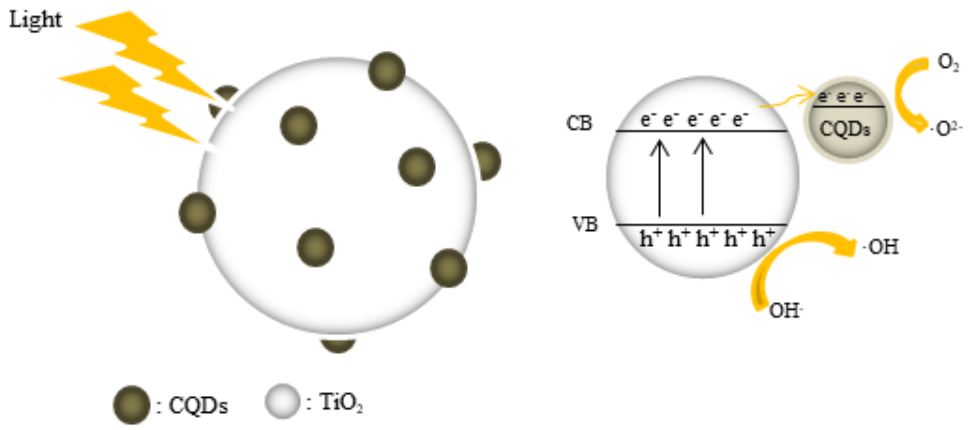

Figure 7. Synergy mechanism of CQD/TiO_2.

Regarding the degradation of naphthalene, the existence of $\cdot O_2^{-}$ and ·OH enable the breaking or cleaving of the ions trapped on CQDs; this leads to the further capture of absorbed O_2 and reactive $\cdot O_2^{-}$ on the hobenzene ring structure. There are two types of hydrogen on the naphthalene structure, namely α-H and β-H (Figure 8). Compared with β-H, α-H has a higher electron density and activity, which means that this site is more easily connected with free radicals. The surface of naphthalene molecules is positively charged, and the electrostatic attraction between atoms can promote the negatively charged ·OH attacks on H at the α position, causing the C at the α position to form hydroxyl derivatives and generate naphthol (products B and C). $\cdot O_2^{-}$ further oxidizes naphthol to form C=O double bonds, forming naphthoquinone (product D). Naphthoquinone is further attacked by ·OH, leading to the cleavage of C–C bonds to form aldehyde compounds. Due to free radical attack at C1 and C4, the resulting aldehyde group is easily oxidized to a carboxyl group, leading to the formation of the product E. These intermediates are further oxidized into smaller molecules and are eventually fully mineralized.

 doi:10.20944/preprints202404.1092.v1

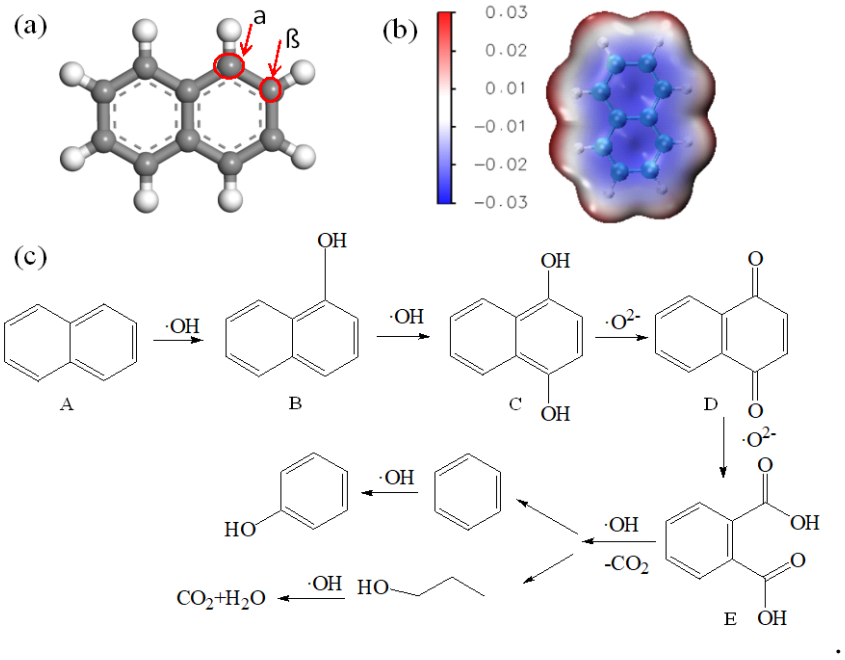

Figure 8. Degradation of naphthalene with CQD/TiO_2: (a) the chemical structure of naphthalene; (b) electrostatic potential (ESP) distribution of naphthalene; (c) degradation pathway map of naphthalene.

3.7. Kinetic Model Analysis of Naphthalene Removal by CQD/TiO_2

The pseudo-first-order kinetic model, the second-order kinetic model, and the double exponential kinetic model were used to fit the photo-catalysis of CQD/TiO_2. The relevant parameters of the kinetic model are shown in Table 1, and the fitting plots can be found in Figure S-6 (Supplementary Material). The results indicated that the pseudo-first-order rate equation provides the best interpretation of the photo-catalysis of naphthalene when the CQD/TiO_2 is used. Meanwhile, the double exponential model provides the best fit for the CQDs, indicating that both physical and chemical processes are involved in the degradation of naphthalene using CQDs, and that a change was experienced after combination with TiO_2. Thus, naphthalene can diffuse thoroughly towards the reaction active site, which accelerates the photo-catalytic reaction.

Table 1. Kinetics parameters for the removal of naphthalene.

Kinetic model	Parameters	CQD/TiO_2	Samples CQD/TiO_2 (dark)	CQDs
Pseudo-first order	k_1x10^2/ (min^{-1})	0.603	0.008	0.104
	R^2	0.8968	0.8608	0.4932
Pseudo-second order	k_2x10^4/ ($L{\cdot}mg^{-1}{\cdot}min^{-1}$)	5.642	0.447	0.552
	R^2	0.7764	0.8480	0.5179
Double exponential	A_1	-41.89	-29.56	-28.14
	A_2	-41.89	-29.56	-28.14
	k_3	0.0588	0.0214	0.1529
	k_4	0.0588	0.0214	0.1529
	R^2	-0.4477	0.2531	0.9150

 doi:10.20944/preprints202404.1092.v1

4. Conclusions

CQDs were prepared using a N,S-containing marine biomass and a simple hydrothermal method, and CQD/TiO_2 composites were synthesized using an ultrasonic method. This work indicated that macroalgae could act as a good precursor for CQDs, whose adsorption and combination performance can be enhanced by dilute sulfuric acid pretreatment; this further enhances the synthesis of CQD/TiO_2 and its photo-catalytic capacity. The nano-structure of CQDs means that they compound well with TiO_2, and thus the photocatalytic performance of TiO_2 can be significantly promoted under this synergistic effect. Generally speaking, the up-conversion performance of CQDs and their tight combination with TiO_2 can be demonstrated by the redshift of the threshold wavelength, a decrease in the binding energy and the further promotion of electron transfer, which enable a better degradation capacity to be achieved under visible light. During the degradation process, CQDs can be used as electron reserves in photocatalysis, thereby promoting the separation efficiency of electron–hole pairs, and further free radicals. They also possess the advantages engendered by biocarbon adsorption due to the intermolecular accumulation of π-π. Therefore, under simulated light irradiation, CQD/TiO_2 exhibits an excellent photocatalytic performance, and the removal of naphthalene is significantly higher than that of simple TiO_2. However, the photo-catalytic efficiency of the composite material seems sensitive to pH, especially during direct recycle tests; however, weak acid treatments can maintain its stability (Figure S-7 in Supplementary Material), which indicates that the more careful modification of acid should be performed in future work.

Supplementary Material: Supplementary data and analysis related to this article can be found online.

This work was supported by the Natural Science Foundation of Zhejiang province (LY20B060008).

References

1. Vijayanand, M., Ramakrishnan, A., Subramanian, R., Issac, P. K., Nasr, M., Khoo, K., Rajagopal, R., Greff, B., Wan, A.N., Jeon, B.H., Chang, S.W., & Ravindran, B. (2023). Polyaromatic hydrocarbons (PAHs) in the water environment: A review on toxicity, microbial biodegradation, systematic biological advancements, and environmental fate. Environmental Research, 115716.
2. Zeng, G., You, H., Du, M., Zhang, Y., Ding, Y., Xu, C., Liu, B., Chen, B. & Pan, X. (2021). Enhancement of photocatalytic activity of TiO_2 by immobilization on activated carbon for degradation of aquatic naphthalene under sunlight irradiation. Chemical Engineering Journal, 412, 128498.
3. Monteiro, F. C., Guimaraes, I. D. L., & Rodrigues, P. D. A. (2023). Degradation of pahs using TiO_2 as a semiconductor in the heterogeneous photocatalysis process: a systematic review. Journal of Photochemistry and Photobiology, A. Chemistry, 437, 114497.
4. Abdel-Latif, H. M., Dawood, M. A., Menanteau-Ledouble, S., & El-Matbouli, M. (2020). Environmental transformation of n-TiO_2 in the aquatic systems and their ecotoxicity in bivalve mollusks: A systematic review. Ecotoxicology and Environmental Safety, 200, 110776.
5. Lettieri, S., Pavone, M., Fioravanti, A., Santamaria Amato, L., & Maddalena, P. (2021). Charge carrier processes and optical properties in TiO_2 and TiO_2-based heterojunction photocatalysts: A review. Materials, 14(7), 1645.
6. Li, F., Liu, G., Liu, F., Wu, J., & Yang, S. (2023). Synergetic effect of cqd and oxygen vacancy to TiO_2 photocatalyst for boosting visible photocatalytic no removal. Journal of Hazardous Materials, 452, 131237.
7. Yu, X., Liu, J., Yu, Y., Zuo, S., & Li, B. (2014). Preparation and visible light photocatalytic activity of carbon quantum dots/TiO_2 nanosheet composites. Carbon, 68, 718-724.
8. [8]García de Arquer, F. P., Talapin, D. V., Klimov, V. I., Arakawa, Y., Bayer, M., & Sargent, E. H. (2021). Semiconductor quantum dots: Technological progress and future challenges. Science, 373(6555), eaaz8541.
9. Zhang, Z., Liu, H., Xu, J., & Zeng, H.(2017). Carbon quantum dots/ biponanocomposites with enhanced visible-light absorption and charge separation. Journal of Photochemistry & Photobiology A Chemistry, 336, 25-31.
10. Pourreza N, Ghomi M. (2019). Green synthesized carbon quantum dots from Prosopis juliflora leaves as a dual off-on fluorescence probe for sensing mercury (II) and chemet drug. Materials Science and Engineering: C, 98(5), 887-896.

 doi:10.20944/preprints202404.1092.v1

11. Das G.S., Shim J.P., Bhatnagar A., Tripathi K.M., & Kim T.Y. (2019). Biomass-derived carbon quantum dots for visible-light-induced photocatalysis and label-free detection of Fe(III) and ascorbic acid. Scientific Reports, 9, 15084.
12. Smetacek V., Adriana Z. (2013). Green and golden seaweed tides on the rise. Nature, 504(7478), 84–88.
13. Zhang, L. Y., Han, Y. L., Yang, J. J., Deng, S. L., & Wang, B. Y. (2021). Construction and photocatalysis of carbon quantum dots/layered mesoporous titanium dioxide (cqds/lm-TiO_2) composites. Applied Surface Science, 546(12), 149089.
14. [14]Piątkowska, A., Janus, M., Szymański, K., & Mozia, S. (2021). C-, N-and S-doped TiO_2 photocatalysts: a review. Catalysts, 11(1), 144.
15. Li, F., Liu, G., Liu, F., Wu, J., & Yang, S. (2023). Synergetic effect of cqd and oxygen vacancy to TiO_2 photocatalyst for boosting visible photocatalytic no removal. Journal of Hazardous Materials, 452, 131237.
16. Khan, M. E., Mohammad, A., & Yoon, T. (2022). State-of-the-art developments in carbon quantum dots (CQDs): Photo-catalysis, bio-imaging, and bio-sensing applications. Chemosphere, 302, 134815.
17. Marković, Z. M., Labudová, M., Danko, M., Matijasević, D., Mičušík, M., Nádaždy, V., Kováčová, M., Kleinová, A., Špitalský, Z., Pavlović, V., Milivojević, D. D., Medić, M. & Marković , B.M. (2020). Highly efficient antioxidant F- and Cl-doped carbon quantum dots for bioimaging. ACS Sustainable Chemistry & Engineering, 8(43), 16327-16338.
18. Cao, F. J., Hou, X., Wang, K. F., Jin, T. Z., & Feng, H. (2023). Facile synthesis of phosphorus and nitrogen co-doped carbon dots with excellent fluorescence emission towards cellular imaging. RSC Advances, 13(30), 21088-21095.
19. Tajik, S., Dourandish, Z., Zhang, K., Beitollahi, H., Le, Q. V., Jang, H. W., & Shokouhimehr, M. (2020). Carbon and graphene quantum dots: a review on syntheses, characterization, biological and sensing applications for neurotransmitter determination. RSC Advances, 10, 15406-15429.
20. Deb, A., & Chowdhury, D. (2024). Biogenic carbon quantum dots: Synthesis and applications. Current Medicinal Chemistry.
21. He, Z., Sun, Y., Zhang, C., Zhang, J., Liu, S., & Zhang, K., & Lan, M. (2023). Recent advances of solvent-engineered carbon dots: a review. Carbon, 204, 76-93.
22. Wareing, T. C., Gentile, P., & Phan, A. N. (2021). Biomass-based carbon dots: current development and future perspectives. ACS Nano, 15(10), 15471-15501.
23. Pinna, M., Binda, G., Altomare, M., Marelli, M., Dossi, C., Monticelli, D., Spanu, D., & Recchia, S. (2021). Biochar nanoparticles over TiO_2 nanotube arrays: A green co-catalyst to boost the photocatalytic degradation of organic pollutants. Catalysts, 11(9), 1048.
24. Nu, T. T. V., Tran, N. H. T., Truong, P. L., Phan, B. T., Dinh, M. T. N., Dinh, V. P., Phan, T.S., Go, S., Chang, M., Trinh, K.T. L., & Van Tran, V. (2022). Green synthesis of microalgae-based carbon dots for decoration of TiO_2 nanoparticles in enhancement of organic dye photodegradation. Environmental Research, 206, 112631.
25. Guo, J., Guo, X., Yang, H., Zhang, D., & Jiang, X. (2023). Construction of Bio-TiO2/Algae Complex and Synergetic Mechanism of the Acceleration of Phenol Biodegradation. Materials, 16(10), 3882.
26. Lai, C., Yang, B., He, J., Huang, C., Li, X., Song, X., & Yong, Q. (2018). Enhanced enzymatic digestibility of mixed wood sawdust by lignin modification with naphthol derivatives during dilute acid pretreatment. Bioresource Technology, 269, 18-24.
27. Ghatak, H. R. (2011). Biorefineries from the perspective of sustainability: Feedstocks, products, and processes. Renewable and Sustainable Energy Reviews, 15(8), 4042-4052.
28. **Zeng, G., Hong, C., Ma, Y., Du, M., Zhang, Y., Luo, H., Chen, B., Pan, X. 2022.** *Sargassum Horneri* based carbon doped TiO_2 and its aquatic naphthalene photo-degradation under sunlight irradiation. *Journal of Chemical Technology and Biotechnology*, 9 7, 1267-1274.
29. Bian, J., Huang, C., Wang, L., Hung, T. F., Daoud, W. A. , & Zhang, R. (2014). Carbon dot loading and tio2 nanorod length dependence of photoelectrochemical properties in carbon dot/tio2 nanorod array nanocomposites. Acs Applied Materials & Interfaces, 6(7), 4883-90.
30. Zhang, L. Y., Han, Y. L., Yang, J. J., Deng, S. L. , & Wang, B. Y. (2021). Construction and photocatalysis of carbon quantum dots/layered mesoporous titanium dioxide (cqds/lm-tio2) composites. Applied Surface Science, 546(12), 149089.
31. Natarajan, S., Bajaj, H., & Tayade, R. (2018) Recent advances based on the synergetic effect of adsorption for removal of dyes from waste water using photocatalytic process. Journal of Environmental Sciences,30, 201-222.
32. Chen, J., Shu, J., Anqi, Z., Juyuan, H., Yan, Z., & Chen, J. (2016). Synthesis of carbon quantum dots/TiO_2 nanocomposite for photo-degradation of Rhodamine B and cefradine. Diamond and Related Materials, 70, 137-144.
33. He, C., Peng, L., Lv, L., Cao, Y., Tu, J., Huang, W., & Zhang, K. (2019). In situ growth of carbon dots on TiO_2 nanotube arrays for PEC enzyme biosensors with visible light response. RSC advances, 9(26), 15084-15091.

 doi:10.20944/preprints202404.1092.v1

34. [34]Chang, L., Ahmad, N., Zeng, G., Ray, A., & Zhang, Y. (2022). N, S co-doped carbon quantum dots/TiO_2 composite for visible-light-driven photocatalytic reduction of Cr (VI). Journal of Environmental Chemical Engineering, 10(6), 108742.
35. Peñas-Garzón, M., Gómez-Avilés, A., Bedia, J., Rodriguez, J. J., & Belver, C. (2019). Effect of activating agent on the properties of TiO_2/activated carbon heterostructures for solar photocatalytic degradation of acetaminophen. Materials, 12(3), 378.
36. Baruah, M., Supong, A., Bhomick, P. C., Karmaker, R., Pongener, C., & Sinha, D. (2020). Batch sorption-photodegradation of Alizarin Red S using synthesized TiO_2 /activated carbon nanocomposite: an experimental study and computer modelling. Nanotechnology for Environmental Engineering, 5, 1-13.
37. [37]Marković, Z. M.,Kováčová, M., Jeremić, S.R., Nagy, Š, Milivojević, D. D., Kubat, P., Kleinová, A., Budimir, M.D., Mojsi, M.M., Stevanović, M.J., Annušová, A., Špitalský, Z., Marković, B. M. T. (2022). Highly efficient antibacterial polymer composites based on hydrophobic riboflavin carbon polymerized dots. Nanomaterials, 12(22), 4070.
38. Liu, J., Zhu, W., Yu, S., & Yan, X. (2014). Three dimensional carbogenic dots/TiO_2 nanoheterojunctions with enhanced visible light-driven photocatalytic activity. Carbon, 2014, 79(11): 369–379.
39. Hu, C., Mu, Y., Li, M., & Qiu, J. (2019). Recent advances in the synthesis and applications of carbon dots. *Acta Physico-Chimica Sinica* , 35(6), 572-590.
40. Sun, X., Li, H. J., Ou, N., Lyu, B., Gui, B., Tian, S., Qian, D., Wang, X., & Yang, J. (2019). Visible-light driven tio photocatalyst coated with graphene quantum dots of tunable nitrogen doping. Molecules (Basel, Switzerland), 24(2).
41. Chang, L., Ahmad, N., **Zeng, G.**, Ray, A., & Zhang, Y. (2022). N, S co-doped carbon quantum dots/TiO_2 composite for visible-light-driven photocatalytic reduction of Cr (VI). Journal of Environmental Chemical Engineering, 10(6), 108742.